

Analysis of seismological data on Reykjanes peninsula, Iceland

Hanna Blanck¹, Philippe Jousset², Gylfi Páll Hersir¹, Kristján Ágústsson¹, Ólafur G. Flóvenz¹

¹ ÍSOR, Iceland Geosurvey, Grensásvegur 9, 108 Reykjavík, Iceland

² GFZ Potsdam, Telegrafenberg, 14473 Potsdam, Germany

hanna.blanck@isor.is

Keywords: IMAGE, seismicity, Reykjanes, Iceland, Vp/Vs.

ABSTRACT

From the spring of 2014 until late 2015 a dense seismic network was recording on Reykjanes Peninsula in southwest Iceland. Additionally to the existing long-term and permanent networks, we deployed a temporary network consisting of 30 on-land stations and 24 Ocean Bottom Seismometers (OBS). The data of the on-land stations were collected every 70 days and the OBSs were read out after recovery. The SeisComp software was used to pick and locate 2066 earthquakes along the mid ocean ridge and within the geothermal system. Earthquakes associated with the geothermal area are very shallow (<2 km) while events along the spreading axis are 4 – 6 km deep on-land and deepening with increased distance from the shore. Furthermore, we see that a cluster of about 200 events which is induced by the drilling on Reykjanes and onset of operation of a local injection borehole. The picked data were used for a Vp/Vs ratio analysis which is an important proxy of porosity, temperature in the subsurface and indicates if partial melt is present. It was calculated to be 1.766 which is consistent with earlier studies of the area. Furthermore, the data can be used as input for various other methods such as travel time, attenuation and ambient noise tomography or interferometry.

1. INTRODUCTION

1.1 Geological setting

The axis of the Atlantic Ocean is formed by the mid-ocean ridge separating the Eurasian and North American plates. The two plates drift apart with a velocity of 1.9 cm a year (Gudmundsson, 1995). Ejected material build a submarine mountain chain reaching up to a height of 3000 m above the

surrounding abyssal planes. About 600 km southeast of Greenland the ridge is overlain by a second geological feature, the Iceland mantle plume (e.g. Pilidou et al., 2014 and references therein). The superposition of the two phenomena and the resulting increase of ejected material since early Tertiary caused the ridge to grow up to 4500 m above the sea floor, forming the island of Iceland.

The Reykjanes peninsula in the southwest of Iceland is the on-land extension of the mid-ocean ridge which forms a band through the island characterized by increased seismic and volcanic activity. Within the volcanic zones in Iceland there are numerous high and low temperature geothermal fields of which 6 are exploited. One of them is the Reykjanes field located at the tip of the Reykjanes peninsula with an installed capacity of about 100 MWe.

The central and western part of the Reykjanes peninsula is covered by hyaloclastite ridges and highly permeable basaltic lava flows (Sæmundsson and Einarsson, 1980). The oldest surface lavas were formed during late Pleistocene, the younger lavas are postglacial and partly historical. The Reykjanes Volcanic belt consists of three volcanic systems, each associated with NE-SW trending fissure swarm, crater rows and hyaloclastic ridges (figure 1). They are intersected by N-S trending right-lateral strike-slip faults (Keiding et al., 2009). Four geothermal areas are found along the fissure swarms, from west to east: Reykjanes, Eldvörp/Svartsengi, Krýsuvík and Brennisteinsfjöll.

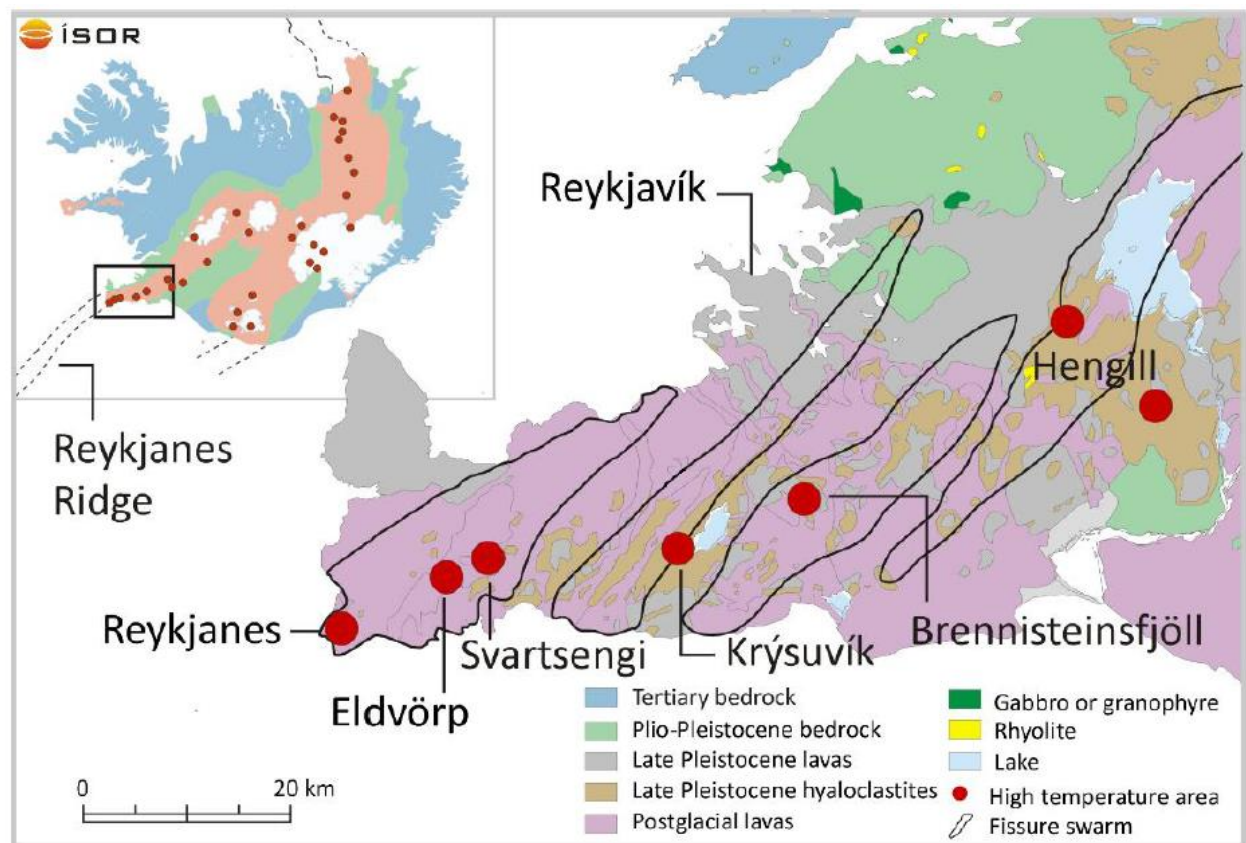


Figure 1: A geological map of Reykjanes peninsula. Four major fissure swarms associated with different volcanic systems and high temperature areas along the ridge are illustrated. The three swarms to the west are located on Reykjanes (based on a geological map by Jóhannesson and Sæmundsson (1999), modified by Harðardóttir et al. (2009).

1.2 Passive seismic in geothermal

For monitoring applications, passive seismology is a valuable tool to follow changes in the local stress field caused by drilling and exploitation processes in geothermal areas. Even though passive seismology is a relatively low cost technique to image the structure of the crust, it has not been used to a great extent for exploration purposes. Detailed velocity information is crucial for successful earthquake analysis. Strong lateral velocity changes have been seen in geothermal areas (e.g. Jousset et al., 2011) making 3D velocity models a necessity for accurate earthquake localization.

This project was part of the EU founded IMAGE (Integrated Methods for Advanced Geothermal Exploration) project. One of the major goals of this project is the improvement of established exploration techniques in geothermal such as ambient noise techniques (e.g. Jousset et al., 2016) and the testing of techniques which are new to this field such the application of a fiber optic cable technique for downhole logging and as a passive strain sensor (Reinsch et al., 2016).

2. THE EXPERIMENT

2.1 The network

In March and April 2014 a seismic network of 30 seismic stations was set up on Reykjanes peninsula by GFZ in Potsdam and Iceland Geosurvey (ÍSOR) in cooperation with HS Orka, the operating energy company on Reykjanes peninsula. It consisted of 20 Trillium Compact Broadband and 10 short-period Mark L-4C seismometers, each installed together with a CUBE datalogger (Omnirecs) which also contains a GPS unit, and a battery for power supply. The data were recorded with a sampling rate of 200 Hz. Additionally, 24 Ocean Bottom Seismometers (OBSs) (sampling rate 100 Hz) were deployed in the Atlantic Ocean around the peninsula by the Alfred Wegener Institute (AWI) together with ÍSOR and GFZ in August the same year. The OBSs completed the network which was laid out as concentric circles around the Reykjanes geothermal system located at the tip of the peninsula (figure 2). Two of the OBSs were caught in fishing nets but they were undamaged and could be redeployed at new locations. After one year of recording, both on-land and off-shore stations,

were retrieved in August 2015. Three of the OBSs could not be recovered.

Additionally, data from other seismic networks in the area were made available. ÍSOR runs a local monitoring network of 8 permanent seismic stations in the Reykjanes geothermal area on behalf of the power company HS Orka, the Czech Academy of Science (CAS) is operating a network of 15 longterm seismic stations in the central and eastern part of the peninsula targeting the Krýsuvík geothermal area and the Icelandic Meteorological Office (IMO) is running 7 stations distributed over the peninsula which are part of the national seismic network monitoring earthquake activity along the mid-ocean ridge and the central volcanoes. Therewith the total number of available seismic stations adds up to 83.

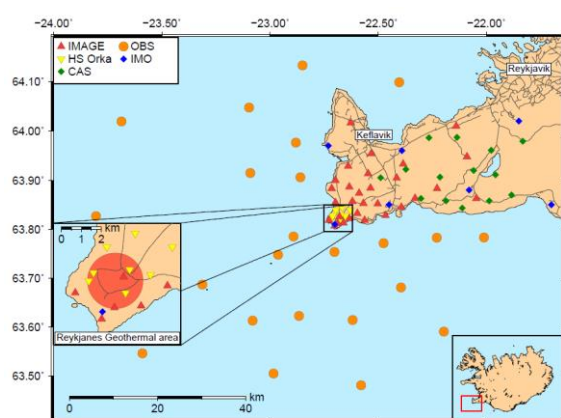


Figure 2: Seismic network on Reykjanes Peninsula as it was recording from 2014 to 2015. The orange filled circles and the red filled triangles represent OBSs and on-land IMAGE stations, respectively. Other seismic stations in the area are the permanent network in Iceland operated by the IMO (blue filled diamonds), the local network in the geothermal area operated by ÍSOR on behalf of HS Orka (yellow filled triangles) and a longterm network monitoring activity in a non-exploited geothermal system in the east of the Reykjanes peninsula operated by CAS (green filled diamonds).

2.2 Installation and maintenance

The Reykjanes peninsula is only sparsely inhabited. Therefore, most of the on-land seismometers could be placed in remote places with no or little man-made noise and even after more than a whole year no station showed signs of unauthorized handling or sabotage. However, the stations are close to the sea shore and a subject to intensive microseism.

The sensors for the on-land stations were placed on bedrock about 60 to 80 cm deep in the ground on a cemented socket (figure 3). They were protected from wind and rain by bottomless plastic barrels which

were buried into the soil. For temperature stabilization the barrel was filled with rock wool. Through an opening on the side of the barrel the seismometer was connected to the data logger and battery which were stored inside a plastic box next to the barrel.

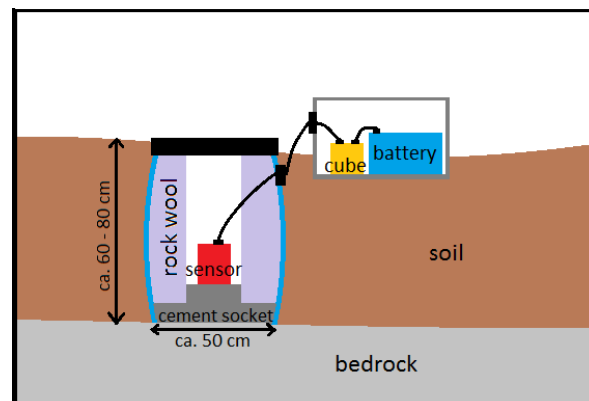


Figure 3: Sketch and example of an IMAGE on-land station. The sensor is placed on bedrock about 70 cm deep in the soil protected by a plastic barrel. The Cube data logger and power supply are in plastic box next to the barrel.

The data of the 30 temporary deployed stations were stored on 16 GB flash hard drives in the CUBES and read-out every two months. Batteries were exchanged at the same time. Locations of the stations were defined with about 1 m accuracy using a differential GPS (Trimble) and the orientation of the seismometers was measured with a Gyrocompass (non-magnetic compass that makes use of the earth's rotation).

3. SEISMICITY

3.1 Historic activity

Reykjanes Peninsula and especially the area around the geothermal system is subject to periodic seismic swarm events. While mainshock/aftershock type swarms are more common in the eastern part of the Reykjanes peninsula, swarms in the western part and at the submarine ridge are typically of continuous activity where no main event can be identified. Such swarms which are lasting usually for a few days were first recorded in 1967 and 1968 when a temporary

network was installed (Ward and Björnsson, 1971). Another swarm of several thousand earthquakes was recorded during a project in 1972 (Klein et al. 1977). The depth of events in these sequences was typically between 2 and 5 km.

The first permanent stations were installed on Reykjanes peninsula by the IMO in 1991 (blue filled diamonds on figure 2). Station RNE at the very tip was added in 2008. Three short seismic swarms in 2006 and another one in 2008 were recorded in this network. In October 2013 a swarm of 880 earthquakes occurred and lasted for 10 days. No significant changes in the surface manifestation of the geothermal system were observed (Guðnason and Ágústsson, 2014).

3.2 Data and processing

All earthquakes were automatically picked using a classic STALTA approach and located with the Seiscomp3 software (www.seiscomp3.org) and later manually revised. A total of 2066 events were located in the network, the vast majority inside the geothermal field and along the mid-ocean ridge. The magnitude of these events rarely exceeded 2 M_L . The manually picked first arrival times of P- and S-phases have been used for travel time tomography (Jousset et al. 2016). Ambient noise techniques have been applied to the data set (Weemstra et al., 2016; Jousset et al. 2016; Verdel et al., 2016).

3.3 Seismic activity

The daily activity is subject to major fluctuations (figure 4). While for more than 58% of the days one or no earthquake was recorded the average number of events recorded per day is 3.9. For 90 % of the days less than 10 earthquakes were recorded.

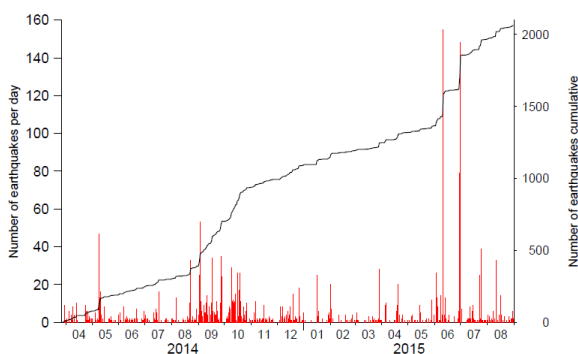


Figure 4: Daily and cumulative number of earthquakes. The number of events per day is subject to strong variations varying between 0 and 155.

About 10 small swarms with 30 or more events lasting one to three days were recorded. The biggest number of earthquakes was recorded on June 11th 2015 when a

swarm consisting of 155 events occurred. The biggest swarm consisted of 227 earthquakes and lasted for two days from June 30th to July 1st.

3.4 Spatial and depth distribution

The vast majority of the earthquakes that were located on and around the Reykjanes peninsula are associated with the Mid-Atlantic rift system entering Iceland at the tip of the peninsula. Most of the events are located at the very tip of the peninsula or in the nearby sea (figure 5) using the SIL model (Bjarnason et al., 1993). All events are currently being relocated using the velocity model derived from this data by Jousset et al. (2016). Along the Reykjanes Ridge with increasing distance from the sea shore the number of events gets smaller and their depths increase. In this area station density and azimuth coverage is less than on land leading to an increase in depth uncertainties. Landwards from the geothermal area events are scarcely scattered but two smaller clusters of events can be identified (marked in figure 5). These clusters are associated with two other geothermal areas on the peninsula, Eldvörp and Svartsengi of which the latter system is exploited and the other is currently explored.

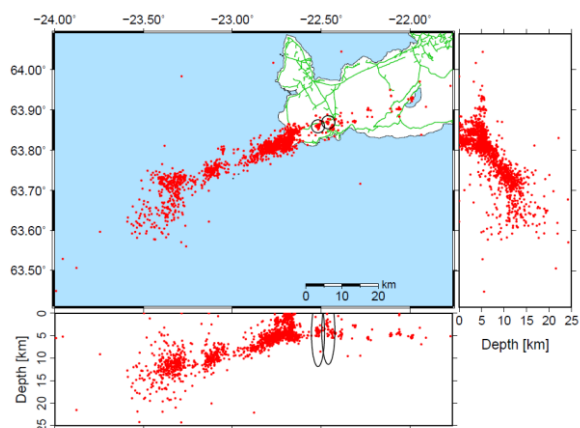


Figure 5: Earthquake distribution. Almost all events are located along the mid-ocean ridge with most events close to the tip of the peninsula. Seawards from the shore the hypocenter depth increases.

A more detailed look at the earthquake distribution at the tip of the peninsula (figure 6) shows that the vast majority of the located earthquakes in the geothermal area itself (productions area and area with presence of surface manifestations) are shallower than 2 km (a). Seismic activity in the crust around the geothermal system, on the other hand, occurs mostly at 4 to 6 km depth (c) and only few events are located at greater depth (d).

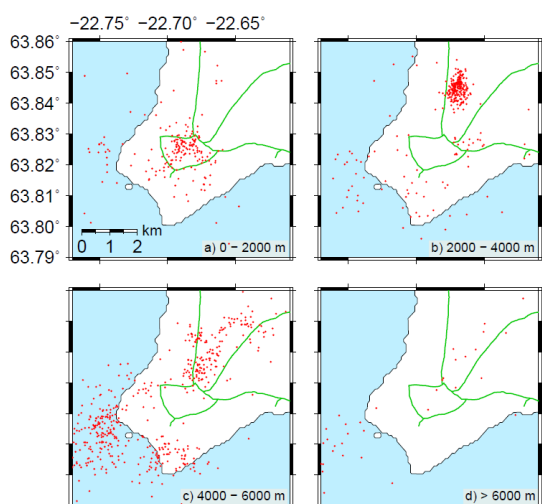


Figure 6: Earthquake distribution within and around Reykjanes geothermal system. Within the area of geothermal surface manifestations events are very shallow (a) while the rifting associated activity is mostly at 4 to 6 km depth (c). In (b) a cluster induced by drilling and operation is visible NE of the geothermal area.

One exception of the observation described above is a cluster located NNE of the main production area where events are concentrated at 2.5 to 3.5 km depth (b). It consists of about 200 events and is not a manifestation of natural activity but is induced by the drilling and starting operation of the injection borehole (RN-34) drilled in February and March 2015.

Apart from the induced cluster whose origin is replicable, there are only few events located at depths between 2.5 and 3.5 km. Here appears to be a clear spatial separation between the rifting related activity and the shallow seismic activity in the geothermal system.

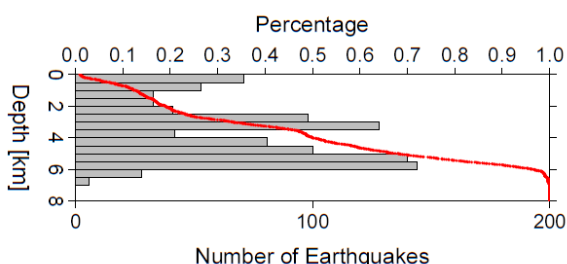


Figure 7: Depth distribution of events at the tip of Reykjanes peninsula (area as plotted in figure 6). There are three discrete active depth ranges from 0 to 1 km, 2.5 to 3.5 km and from 4 to 6 km.

The depth distribution derived from events at the tip of the peninsula only (figure 7) clearly shows these three main depth ranges of activity. There is an increased number of events that were located very shallow (<1 km), the induced cluster at 2.5 to 3.5 km depth and the rifting associated activity at 4 to 6 km depth. In this area no earthquake is located deeper than 7 km.

These different depth ranges are also reflected in the depth distribution derived from all located events (figure 8). Here another active depth range between 9 and 14 km is visible.

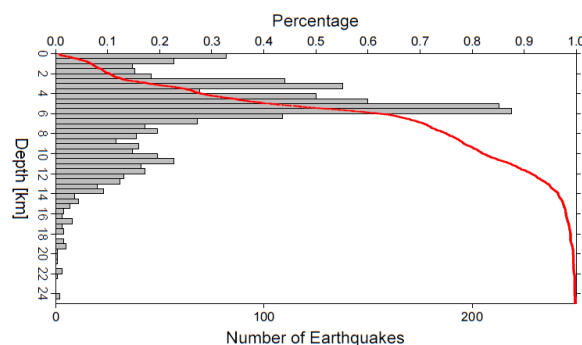


Figure 8: Depth distribution of all recorded events. The active depth ranges seen in figure 7 are still dominant. Increased activity is further present between 9 and 14 km.

4. VELOCITY RATIO

The picked P- and S-wave arrival times of the located earthquakes were used to estimate the V_p/V_s ratio using a Wadati diagram (Wadati, 1933) which averages the velocity ratio along the wave travel path. This approach assumes that the Poisson's ratio is constant which results in equal ray paths of both P- and S-wave.

The V_p/V_s ratio was calculated to be 1.766 ± 0.001 (Figure 9). This value is in agreement with earlier studies on this part of the Icelandic crust which show values of about 1.74 – 1.79 (e.g. Brandsdóttir and Menke, 2008, and references therein, Weir et al., 2001) and indicates temperatures below solidus with little or no partial melt present (Brandsdóttir and Menke, 2008). This would be consistent with the fact that no big or shallow magma chamber is known in the area.

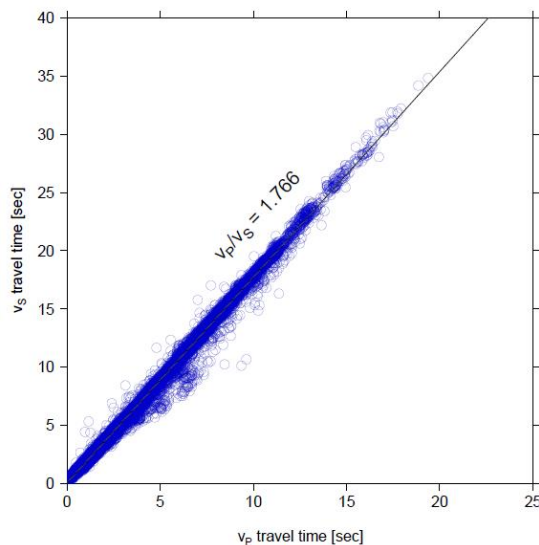


Figure 9: V_p/V_s ratio derived from picked arrival times from all 2066 events. The ratio is 1.766 ± 0.001 , slightly higher than standard crustal values but in consent with earlier studies on Reykjanes peninsula and the Icelandic south.

5. DISCUSSION AND OUTLOOK

The Reykjanes Geothermal field, which has been exploited since 2006 with capacity of 100 MWe, has been seismically monitored since 2013. In this study, the seismic activity recorded between March 2014 and August 2015 was analyzed when the permanent network in the geothermal area consisting of 8 stations was expanded by 30 temporarily on-land and 24 Ocean Bottom Seismometers. Additionally, the data of 22 stations from other networks in the region were made available. A total of 2066 earthquakes could be recorded and located.

The analysis of the spatial and depth distribution of the events at Reykjanes shows that the main activity is limited to two depth ranges. Inside the geothermal area events are mostly located at less than 2 km depth. In the nearby surrounding crust another more active layer is visible which reaches from 4 km to 6 km. An exception to these two layers of activity is a locally limited cluster reaching from a depth of 2.5 to 3.5 km depth which is associated with injection in borehole RN-34 which was drilled in early 2015 and reaches down to 2.6 km depth. The earthquake distribution clearly shows the boundaries of the temperature anomaly in the upper crust which corresponds to the surface manifestations in the area.

The lower active depth layer (4 - 6 km depth) surrounding the geothermal area is associated with the Mid-Atlantic ridge running through Iceland where it forms a volcanically and seismically active zone. In the sea the depth to this layer is increasing with distance from the shore where the brittle-ductile boundary reaching as deep as 10 km. This is

consistent with e.g. the Kolbeinsey ridge in the north of Iceland. Here earthquakes are typically in the depth range of 2 to 6 km close to the ridge (Rögnvaldsson et al. 1998) and down to a depth of 12 km with greater distance from the spreading centre while shallower events are only rarely observed.

Different tomography technique such as double-differences, ambient noise and attenuation tomography have been performed or are work in progress. The earthquakes will be relocalized with the new velocity models from the tomography using double-differences relocalization. Moment tensor inversion and ambient noise interferometry is currently being worked on.

REFERENCES

- Bjarnason, I. Th., Menke, W., Flóvenz, Ó. G. and Caress, D.: Tomographic image of the Mid-Atlantic Plate Boundary in southwestern Iceland. *J. Geophys. Res.*, **98**, (1993), 6607–6622.
- Brandsdóttir, B. and Menke, W.: The seismic structure of Iceland, *Jokull*, **58**, (2008), 17-34.
- Gudmundsson, A.: Ocean-ridge discontinuities in Iceland, *J. Geol. Soc.*, **152**, (1995), 1011-1015.
- Gudnason, E. and Ágústsson, K.: Earthquake swarm on Reykjanes in October 2013, *ÍSOR*, Reykjavík, (2014).
- Harðardóttir, V., Brown, K. L., Friðriksson, Th., Hedenquist, J. W., Hannington, M. D. and Thórhallsson, S.: Metals in deep liquid of the Reykjanes geothermal system, southwest Iceland: Implications for the composition of seafloor black smoker fluids, *Geology*, v. **37**, no. 12, (2009), 1103-1106.
- Reinsch, T., Jousset, P., Hennings, J. and Blanck, H.: Distributed Acoustic Sensing Technology in Magmatic Areas – First Results from a Survey in Iceland, *Proceedings of the European Geothermal Congress 2016*, Strasbourg, France, (2016), September 2016.
- Jousset, P., Haberland, C., Bauer, K., and Arnason, K.: Hengill geothermal volcanic complex (Iceland) characterized by integrated geophysical observations. *Geothermics*, **40**, (2011), 1–24.
- Jousset, P., Blanck, H., Franke, S., Agustsson, K., Metz, M., Ryberg, T., Hersir, G., Weemstra, C., Verdel, A., Bruhn, D.: Seismic tomography of Reykjanes, SW Iceland, *Proceedings of the European Geothermal Congress 2016*, Strasbourg, France, (2016), September 2016.
- Keiding, M., Lund, B. and Árnadóttir, Th.: Earthquakes, stress and strain along an obliquely divergent plate boundary: the Reykjanes Peninsula, southwest Iceland, *J. Geophys. Res.*, **114**, (2009), B09306.

- Klein, F. W., Einarsson, P. and Wyss, M.: The Reykjanes Peninsula Iceland, earthquake swarm of September 1972 and its tectonic significance, *J. Geophys. Res.*, **82**, (1977), 865-888.
- Pilidou, S., Priestley, K., Gudmundsson, Ó. and Debayle, E.: Upper mantle S-wave speed heterogeneity and anisotropy beneath the North Atlantic from regional surface wave tomography: the Iceland and Azores plumes, *Geophysical Journal International*, **159**, (2004), 1057-1076.
- Rögnvaldsson, S. Th., Gudmundsson, A. and Slunga, R.: Seismotectonic analysis of the Tjörnes fracture zone – an active transform fault in North Iceland, Icelandic Meteorological Office, Reykjavík, (1998).
- Sæmundsson, K. and Einarsson, S.: Geological map of Iceland, sheet 3, SW-Iceland, second edition, 1:250 000, (1980).
- Verdel, A., Wedemeijer, H., Paap, B., Vandemeijer, V., Weemstra, C., Jousset, P., Franke, S., Blanck, H., Ágústsson, K. and Hersir, G.P.: Reykjanes ambient noise reflection interferometry, *Proceedings of the European Geothermal Congress 2016*, Strasbourg, France, (2016), September 2016.
- Wadati, K.: On travel time of earthquake waves. *Geophys. Mag.*, **7**, (1933), 101–111.
- Ward, P. and Björnsson, S.: Microearthquakes, swarms and the geothermal areas of Iceland, *J. Geophys. Res.*, **76**, (1971), 3953-3982.
- Weird, N., White, R., Brandsdóttir, B., Einarsson, P., Shimamura, H., Shiobara, H. and the RISE Fieldwork Team.: Crustal structure of the northern Reykjanes Ridge and Reykjanes Peninsula, southwest Iceland, *Journal of Geophysical Research*, **106**, (2001), 6347-6368.
- Weemstra, C., Obermann, A., Verdel, A., Paab, B., Blanck, H., Gudnason, E.Á., Hersir, G.P., Jousset, P. and Sigurdsson, Ó.: Time-lapse seismic imaging of the Reykjanes geothermal reservoir, *Proceedings of the European Geothermal Congress 2016*, Strasbourg, France, (2016), September 2016.
- Methods for Advanced Geothermal Exploration (IMAGE)).
- The project was supported by the energy company HS Orka, which is a part of the IMAGE consortium. The Icelandic Meteorological Office provided the data of the SIL stations on the Reykjanes peninsula. The Czech Academy of Science (CAS) provided the data of the REYKJANET network. Their contribution is acknowledged.
- We would like to thank Guðrún Ósk Sæmundsdóttir, Mykola Khyzhnyak, Sif Pétursdóttir and Sigrún Tómasdóttir for the manual revision of the waveform picks and localizations as well as Stefán Auðunn Stefánsson and Kemal Erbas for their participation in setup and maintenance of the seismic network.

Acknowledgements

The instruments used in this project were provided by the GIPP (Geophysical instrumental Pool of Potsdam) and the DEPAS (Deutsche Geräte Pool für Amphibische Seismologie).

The research leading to these results has received funding from the EC Seventh Framework Programme under grant agreement No. 608553 (project Integrated

Table 1: List of seismic stations. IMAGE and OBS stations were temporarily, CAS longterm and HS Orka and IMO stations are a part of permanently installed networks. SP – Short Period, BB – Broadband, IM – Intermediate.

Network	Station	Type	Lat [°]	Lon [°]	Sensor	Datalogger
IMAGE	ARN	SP	63,862844	-22,046070	Mark Sensor	CUBE
	BER	BB	63,818466	-22,562944	Trillium Comp	CUBE
	EIN	BB	63,856934	-22,619266	Trillium Comp	CUBE
	GEV	BB	63,828094	-22,466464	Trillium Comp	CUBE
	HAH	BB	63,928601	-22,638602	Trillium Comp	CUBE
	HAS	BB	63,882949	-22,715219	Trillium Comp	CUBE
	HOP	SP	63,845073	-22,392420	Mark Sensor	CUBE
	HOS	BB	63,947675	-22,089654	Trillium Comp	CUBE
	KEF	BB	64,016213	-22,627548	Trillium Comp	CUBE
	KHR	SP	63,832367	-22,596432	Mark Sensor	CUBE
	KRV	SP	63,812744	-22,660527	Mark Sensor	CUBE
	KUG	BB	64,009625	-22,139352	Trillium Comp	CUBE
	LFE	BB	63,883868	-22,535548	Trillium Comp	CUBE
	MER	SP	63,883236	-22,228253	Mark Sensor	CUBE
	NEW	SP	63,932983	-22,385217	Mark Sensor	CUBE
	ONG	BB	63,818635	-22,727764	Trillium Comp	CUBE
	PAT	BB	63,953996	-22,532067	Trillium Comp	CUBE
	PRE	BB	63,886239	-22,633366	Trillium Comp	CUBE
	RAH	BB	63,852855	-22,567946	Trillium Comp	CUBE
	RAR	BB	63,825801	-22,678329	Trillium Comp	CUBE
	RET	BB	63,806753	-22,700812	Trillium Comp	CUBE
	SDV	BB	63,821768	-22,633443	Trillium Comp	CUBE
	SKF	SP	63,811928	-22,687782	Mark Sensor	CUBE
	SKG	BB	63,863371	-22,329210	Trillium Comp	CUBE
	SKH	BB	63,904584	-22,414933	Trillium Comp	CUBE
	STA	BB	63,854302	-22,697544	Trillium Comp	CUBE
	STF	SP	63,913445	-22,547067	Mark Sensor	CUBE
	STK	SP	63,899571	-22,697866	Mark Sensor	CUBE
	SUH	BB	63,852128	-22,502155	Trillium Comp	CUBE
	VSR	SP	63,873686	-22,588137	Mark Sensor	CUBE
HS Orka	ELBDG	SP	63,823890	-22,714010	LE-3Dlite	Reftek 130
	GUNN	SP	63,818625	-22,676450	LE-3Dlite	Reftek 130
	LANG	SP	63,826730	-22,650670	LE-3Dlite	Reftek 130
	STMN	SP	63,841960	-22,694360	LE-3Dlite	Reftek 130
	STMS	SP	63,827630	-22,709080	LE-3Dlite	Reftek 130
	SYRA	SP	63,839280	-22,628520	LE-3Dlite	Reftek 130
	SYRD	SP	63,824280	-22,680610	LE-3Dlite	Reftek 130
	SYRN	SP	63,845430	-22,666520	LE-3Dlite	Reftek 130

CAS	ASH	SP	63,987083	-22,136117	LE-3D	Vistec/Gaia
	FAF	IM	63,906420	-22,214830	CMG-40T	Vistec/Gaia
	HRG	IM	63,960580	-21,977840	CMG-40T	Vistec/Gaia
	KLV	IM	63,911250	-21,958230	CMG-40T	Vistec/Gaia
	LSF	IM	63,922240	-22,372230	CMG-40T	Vistec/Gaia
	SEA	SP	63,843310	-22,111090	LE-3D	Vistec/Gaia
	ELB	IM	63,858180	-21,987210	CMG-40T	Vistec/Gaia
	GEI	SP	63,948180	-21,530700	LE-3D	Vistec/Gaia
	HDV	SP	63,869600	-21,883450	LE-3D	Vistec/Gaia
	ISS	SP	63,862930	-22,302940	LE-3D	Vistec/Gaia
	LAG	SP	63,904850	-22,488460	LE-3D	Vistec/Gaia
	LAT	IM	63,858240	-22,186900	CMG-40T	Vistec/Gaia
	LHL	IM	63,979100	-21,832070	CMG-40T	Vistec/Gaia
	MOH	IM	63,919830	-22,059400	CMG-40T	Vistec/Gaia
	STH	IM	63,986430	-22,265160	CMG-40T	Vistec/Gaia
OBS stations	OBS01	IM	63,783440	-22,011420	CMG-40T	
	OBS02	IM	63,783400	-22,228670	CMG-40T	
	OBS03	IM	63,771560	-22,474740	CMG-40T	
	OBS04	IM	63,753810	-22,700600	CMG-40T	
	OBS05	IM	63,772840	-22,840960	CMG-40T	
	OBS06	IM	63,905640	-22,859410	CMG-40T	
	OBS07	IM	63,976133	-22,880250	CMG-40T	
	OBS08	IM	64,098200	-22,402900	CMG-40T	
	OBS09	IM	64,132430	-22,849670	CMG-40T	
	OBS10	IM	64,047050	-23,096510	CMG-40T	
	OBS11	IM	63,915000	-23,091000	CMG-40T	
	OBS12	IM	63,776530	-23,251420	CMG-40T	
	OBS13	IM	63,747940	-22,962910	CMG-40T	
	OBS14	IM	63,622760	-22,866040	CMG-40T	
	OBS15	IM	63,614220	-22,618400	CMG-40T	
	OBS16	IM	63,681140	-22,394370	CMG-40T	
	OBS17	IM	63,591020	-22,196840	CMG-40T	
	OBS18	IM	63,280180	-22,579460	CMG-40T	
	OBS19	IM	63,613030	-23,079990	CMG-40T	
	OBS20	IM	63,687190	-23,312530	CMG-40T	
	OBS21	IM	64,018890	-23,686300	CMG-40T	
	OBS22	IM	63,826790	-23,803730	CMG-40T	
	OBS23	IM	63,504390	-22,983520	CMG-40T	
	OBS24	IM	63,586380	-23,504510	CMG-40T	
	OBS25	IM	63,785400	-22,890780	CMG-40T	
	OBS26	IM	63,545960	-23,589810	CMG-40T	
IMO	GRV	SP	63,857160	-22,455830	LE-3D5s	Guralp DM24
	KAS	SP	64,022900	-21,852000	LE-3D5s	Guralp DM24
	KRI	SP	63,878100	-22,076460	LE-3D1s	Guralp DM24
	NYL	SP	63,973680	-22,737680	LE-3D5s	Guralp DM24
	RNE	SP	63,816810	-22,705630	LE-3D5s	Guralp DM24
	VOG	BB	63,969670	-22,392850	Guralp CMG3ESPB	Guralp DM24
	VOS	SP	63,852790	-21,703570	LE-3D5s	Guralp DM24